frontiers in Environmental Chemistry

ORIGINAL RESEARCH
published: 15 April 2021
doi: 10.3389/fenvc.2021.670431

One-Pot Synthesis of CeO_2 Modified SBA-15 With No Pore Clogging for NO Reduction by CO

Kaili Ma[1], *Hongliang Zhang*[2]*, *Changjin Tang*[3]* and *Lin Dong*[4]

[1] Analysis and Testing Center, Southeast University, Nanjing, China, [2] Analysis and Testing Central Facility, Anhui University of Technology, Maanshan, China, [3] School of Environment, Nanjing Normal University, Nanjing, China, [4] Jiangsu Key Laboratory of Vehicle Emissions Control, Center of Modern Analysis, School of the Environment, Nanjing University, Nanjing, China

CeO_2 modified SBA-15 composites have been prepared by adding cerium precursor ($Ce(NO_3)_3{\cdot}6H_2O$) directly into the mixture of soft template (P123), silica precursor (TEOS) and urea aqueous solution but without mineral acid. The products were characterized by X-ray fluorescence (XRF), powder X-ray diffraction (XRD), N_2 physisorption and transmission electron microscopy (TEM). Results indicated that ceria were successfully grafted onto mesoporous silica matrix and no pore clogging was observed. Both ceria content and mesoporous ordering of the final products were found to depend on urea amount. Compared to CeO_2/SBA-15 from conventional impregnation method, the one-pot synthesis not only showed simple and green operation, but also superior catalytic performance in NO+CO reaction after loaded with CuO. It was revealed that both the presence and location of ceria had great influence on the reducibility of CuO, and the catalytic performances were intimately related to the redox properties of crystalline CuO. That is, higher NO conversion and N_2 selectivity were achieved over catalyst with easier reduction of crystalline CuO.

Keywords: CeO_2/SBA-15 composites, one-pot synthesis, redox properties, NO+CO reaction, pore clogging

OPEN ACCESS

Edited by:
Dengsong Zhang,
Shanghai University, China

Reviewed by:
Xiaodong Zhang,
University of Shanghai for Science and Technology, China
Yuechang Wei,
China University of Petroleum, China

***Correspondence:**
Hongliang Zhang
zhanghl@ahut.edu.cn
Changjin Tang
tangcj@njnu.edu.cn

Specialty section:
This article was submitted to Catalytic Remediation, a section of the journal Frontiers in Environmental Chemistry

Received: *21 February 2021*
Accepted: *19 March 2021*
Published: *15 April 2021*

Citation:
Ma K, Zhang H, Tang C and Dong L (2021) One-Pot Synthesis of CeO_2 Modified SBA-15 With No Pore Clogging for NO Reduction by CO. Front. Environ. Chem. 2:670431. doi: 10.3389/fenvc.2021.670431

INTRODUCTION

Ceria and ceria-based materials have received numerous attention in heterogeneous catalysis, particularly in the field of environmental catalysis, such as CO oxidation (Slavinskaya et al., 2020), NO reduction (Tang et al., 2016), soot oxidation (Wang et al., 2021), and elimination of VOCs (Shi et al., 2021). In order to improve the performances, preparation of ceria or related materials with designed structures and morphologies is extensively investigated (Liang et al., 2008; Wei et al., 2011; Ta et al., 2012; Ma et al., 2017; Wu et al., 2018; Ri et al., 2021), and this has become a hot research topic with the rapid development of material preparation techniques (Li and Shen, 2014; Trovarelli and Llorca, 2017; Bi et al., 2020). In principle, creation of structured materials with large surface area is much attractive since it can provide abundant active sites and sufficient anchoring sites for better dispersion of active species. This is typically realized by preparing ceria or ceria-based materials with mesoporous structures (Qi et al., 2012; Tang et al., 2015; Zhan et al., 2017). For example, Shen et al. (2005) and Luo et al. (2007) reported the synthesis of mesoporous CeO_2 by hard and soft template methods, respectively. Meanwhile, the catalytic performances in CO oxidation were evaluated. Results showed that mesoporous ceria was more active than regular ceria from cerium(III) nitrate decomposition and the catalytic activities were greatly enhanced for

CuO-loaded catalysts. Nevertheless, it was noteworthy that their textual stability was not very good at high temperatures.

As an alternative, ordered mesoporous CeO_2-SiO_2 composites attract great interest due to the fact that the ordered mesoporous SiO_2 matrix could not only improve textural stability of CeO_2 but also possess large surface area. The conventional method of obtaining ordered mesoporous CeO_2/SiO_2 is impregnation of mesoporous silica materials, i.e., MCM-41 (Akondi et al., 2012) and SBA-15 (Mikheeva et al., 2019), with cerium salts. By this method, agglomeration of ceria particles is usually occurred and the blocking of mesopores is inevitable (Bi et al., 2007; Krishnan et al., 2008). There was alternative method reported for preparation of finely dispersed ceria in CeO_2/SiO_2 composite (Corma et al., 2004). The first step was synthesis of uniformly distributed ceria nanoparticles and then introduced them into the synthesis system of SBA-15. For both methods, at least two steps are involved, which are time consuming and not advantageous in the view of simplicity. There were also few reports concerning on direct synthesis of ordered mesoporous CeO_2/SiO_2 (Khalil, 2007; Li et al., 2009). For example, Li et al. prepared CeO_2/SiO_2 mesostructured composite through an evaporation induced self-assembly (EISA) strategy (Li et al., 2009). However, the synthesis parameter should be strictly controlled as it needs to be operated at restricted humidity. Moreover, the pore volume is found to be apparently decreased, suggesting the occurrence of obvious pore clogging.

For the preparation of mesoporous CeO_2/SiO_2 composite, it is highly expected that the guest species can be directly introduced into mesoporous matrix throughout the preparation. More importantly, to accelerate stream diffusion and promote active site exposure, apparent pore clogging should be avoided. As for silica matrix, SBA-15 is more often used than MCM-41, mainly due to its thicker pore wall and larger pore size. However, since SBA-15 is usually prepared in strong acidic condition, it is hard to introduce guest species directly into the mesoporous matrix. This may account for the well-known fact that most preparation of CeO_2/SBA-15 composites involve two steps. In the present study, a novel and facile one-pot synthesis method of ceria modified SBA-15 was investigated. The products were prepared by directly adding cerium precursor into the mixture of P123, TEOS and urea aqueous solution. The physicochemical properties of samples were characterized by XRF, XRD, N_2 adsorption/desorption, and TEM. In contrast to the counterpart from wet impregnation, it is interesting that for the samples from one-pot synthesis, no pore clogging is observed. Moreover, much higher catalytic activity over NO+CO reaction is obtained after loaded with CuO, suggesting the great potential of this method in fabricating CeO_2-mesoporous silica composites.

EXPERIMENTAL

Sample Preparation

Synthesis of CeO_2@SBA-15

The one-pot synthesis of CeO_2 modified SBA-15 was based on modification of our previous work (Zhang et al., 2012). In a typical synthesis procedure, 2 g of P123 was dissolved in 50 mL of distilled water under stirring. Then a certain amount of urea and 0.88 g of $Ce(NO_3)_3{\cdot}6H_2O$ were added to the template solution. After stirred at 40°C for 0.5 h, 4.25 g of TEOS was dropped and the mixture was kept stirring for 24 h, and then subjected to hydrothermal treatment in an autoclave at 100°C for 24 h. The solid product was recovered by filtration, washed with distilled water and ethanol, and dried at room temperature. Finally, it was air-calcined to 550°C at the ramp rate of 1°C/min and maintained for 6 h to remove the template. For convenience, the obtained samples were denoted as CeO_2@SBA-15(*m*) where *m* represented the mass of urea added in terms of gram. For comparison, the CeO_2/SBA-15 was prepared by wet impregnation and the ceria loading was set at the same value with that in CeO_2@SBA-15(0.8).

To illuminate the formation process of the one-pot method, two controlled experiments were designed based on minor modification of the synthetic procedure to CeO_2@SBA-15. (i) Synthesis of CeO_2@SBA-15 without the addition of urea and the obtained sample was denoted as CS-1; (ii) Synthesis of CeO_2@SBA-15 (0.8) without the hydrothermal process at 100°C and the obtained sample was denoted as CS-2.

Preparation of CuO-Loaded Catalysts

In order to investigate the catalytic performance of CeO_2 modified SBA-15, the CuO-loaded catalysts were prepared. The CuO-loaded sample was prepared by impregnating CeO_2@SBA-15(0.8) with an aqueous solution containing requisite amount of copper(II) nitrate trihydrate [$Cu(NO_3)_2{\cdot}3H_2O$], followed by drying at 110°C overnight and then calcining in air at 550°C for 6 h at a ramp rate of 1°C/min. The CuO-loaded catalyst was labeled as CuO/CeO_2@SBA-15. For comparison, other two CuO-loaded catalysts were prepared with the same procedure and denoted as CuO/CeO_2/SBA-15 and CuO/SBA-15, respectively.

Characterization

The powder X-ray diffraction patterns of samples were collected on a Philips X'pert X-ray diffractometer using Ni-filtered Cu K_α radiation ($\lambda = 0.15418$ nm). The X-ray tube was operated at 40 kV and 40 mA. The average grain size of ceria was determined by Sherrer equation from the (220) crystalline plane of ceria.

Nitrogen adsorption and desorption isotherms were measured at −196°C using a Micromeritics ASAP 2020 system. The samples were degassed for 160 min at 300°C in the degas port of the adsorption analyzer. The pore size distribution (PSD) curves were calculated from the analysis of the desorption branch of the isotherms using the Barrett-Joyner-Halenda (BJH) algorithm.

Ceria contents in the samples were determined by X-ray fluorescence (XRF) using an ARL-9800 spectrometer. The composition of samples was measured by balancing the oxygen content in every specimen and determining the total weight amount of SiO_2 and CeO_2 in every sample. The preservation rate of ceria was devised as a reference to determine the effect of urea addition based on XRF results and the detailed meaning was defined as follows:

$$\text{Preservation rate of ceria}(\%) = \frac{\text{ceria content in the sample}}{\text{amount of cerium added in terms of ceria}} \times 100$$

Transmission electron microscopy (TEM) images were taken on a JEM-2100 instrument at an acceleration voltage of 200 kV. The samples were crushed in A.R. grade ethanol and the resulting

suspensions were allowed to dry on carbon film supported on copper grids.

H_2 temperature-programmed reduction (H_2-TPR) measurements were carried out in a quartz U-type reactor connected to a thermal conduction detector (TCD) with a H_2-Ar mixture (7.3% H_2 by volume) as reductant. 25 mg of sample was used for each measurement. Before switched to the H_2-Ar stream, the sample was pretreated in N_2 stream at 100°C for 1 h. Each TPR measurement started from room temperature to 450°C at a ramp rate of 10°C/min.

Catalytic Activity Test

The activities in NO+CO reaction were determined under steady state, involving a feed stream with a fixed composition, 5% NO, 10% CO, and 85% He by volume as diluents. A quartz tube with 25 mg catalyst was used. The catalysts were pretreated in N_2 stream at 100°C for 1 h and then cooled to room temperature, after that, the gas reactants were switched on. The reaction was carried out at different temperatures with a space velocity of 24,000 mL g^{-1} h^{-1}. Two columns and thermal conduction detection (TCD) were used for separating and analyzing the products, respectively. Column A with Paropak Q for separating N_2O and CO_2, and column B, packed with 5A and 13X molecular sieves (40–60 mesh) for separating N_2, NO and CO.

RESULTS AND DISCUSSION

Physicochemical Properties of CeO_2@SBA-15

To explore the effectiveness of one-pot synthesis, the information of ceria content in CeO_2@SBA-15 was firstly investigated and the results of XRF are presented in **Figure 1**. From **Figure 1**, it is found that ceria is more or less preserved in the final products, which is determined by the amount of urea used. With addition of the least amount of urea (0.2 g), < 40% ceria is kept back as comparing the measured ceria with nominal amount. However, when increasing the urea amount to 0.8 g, > 80% of the precursor is saved in the product. Noticeably, further increasing urea amount leads to the preservation rate decreased to 66%.

The formation of ordered mesoporous structures was studied by small angle XRD (SAXRD). **Figure 2** shows the effect of urea amount on the SAXRD patterns of CeO_2@SBA-15. As a reference, the pattern of CeO_2/SBA-15 is presented. For all samples, one intense and two weak peaks are observed, which can be indexed into the (100), (110), and (200) reflections of the hexagonal space group *p6mm*, suggesting that the typical hexagonal structure of SBA-15 has been obtained throughout the synthesis and subsequent calcination. By further examining the dominant peak of CeO_2@SBA-15, it is found that the position of (100) reflection is almost not shifted, implying the unit-cell parameter of mesoporous framework is not affected by the amount of urea added. Nevertheless, the signal intensity, which is related to the ordering of mesoporous structure, grows weaker with increased urea amount. With the maximal urea added, the mesoporous ordering is obviously disturbed, as evidenced by the appearance of indefinite higher order peaks in the corresponding pattern. Based on these results, we can conclude that well-ordered

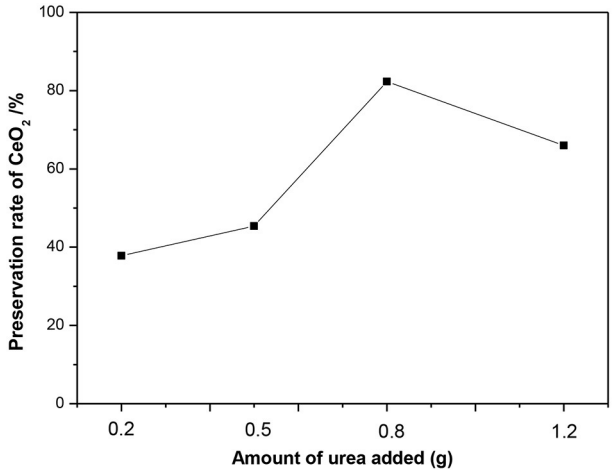

FIGURE 1 | The preservation rate of ceria as a function of urea added for different samples.

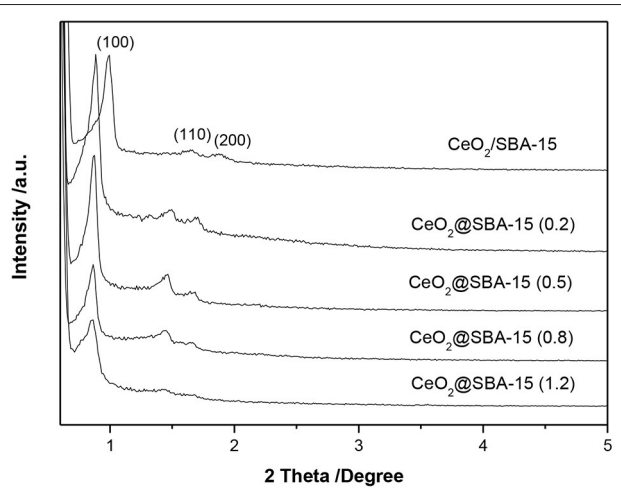

FIGURE 2 | The small angle XRD patterns of different ceria loaded samples.

ceria modified SBA-15 composites are successfully prepared by the one-pot synthesis. On the other hand, by comparing the patterns of samples from different methods, it is obvious that the one-pot prepared samples have larger unit-cell parameters than the impregnated one.

In previous study, it was reported that for some multivalent metal ions, *e.g.*, Mo^{6+}, they could induce the assembly of SBA-15 framework through interaction with P123 template (Zhang et al., 2012). This may also hold true for cerium as reflected by the SAXRD pattern (**Supplementary Figure 1**). The appearance of three diffraction peaks clearly indicated that highly ordered hexagonal mesostructures were obtained for CS-1 sample. However, as can be seen from **Supplementary Figure 2**, the final product without urea addition (CS-1) was almost free of cerium. This is not advantageous for direct functionalization of SBA-15. Fortunately, the weakness was overcome by employing urea into the synthesis system. An explosion of ceria content

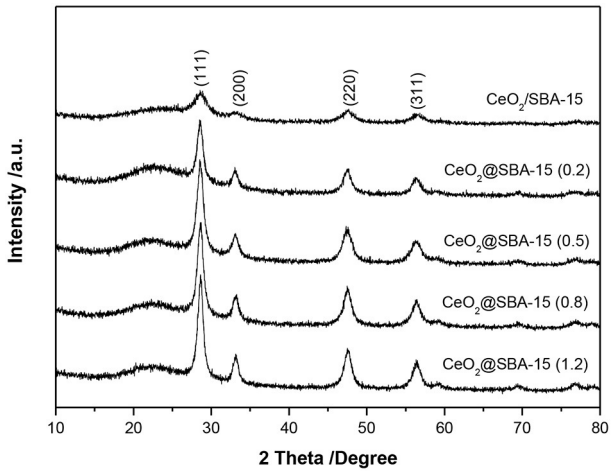

FIGURE 3 | The wide angle XRD patterns of different ceria loaded samples.

is observed for CeO_2@SBA-15 (**Supplementary Figure 2**). The unique property of urea in generating ammonia at elevated temperature ($> 80^{\circ}C$) is supposed to play the key role in realizing one-pot modification of SBA-15 with ceria. That is, the preliminary formation of rigid mesoporous framework (pattern of CS-2 in **Supplementary Figure 1**) and subsequent grafting guest species onto silica matrix through *in situ* modulation of synthesis pH from urea decomposition. Additionally, it is noteworthy that the amount of urea addition influences ordering of the final products. With increasing of urea amount, more ammonia would be produced. Consequently, the pH value of synthesis medium increases and the ordering of the mesoporous structures is resultantly disturbed (Escas et al., 2007).

The phase and phase purity of mesoporous CeO_2/silica hybrids were investigated by wide angle XRD and results are filed in **Figure 3**. For all samples, broad reflection in the region of 20–26° belongs to amorphous silica. The diffraction peaks at $2\theta = 28.6^{\circ}$, 33.1°, 47.5°, and 56.3°, corresponding to d spacing of 3.12, 2.71, 1.91, and 1.63 Å characteristic of the (111), (200), (220), and (311) plane of CeO_2 crystallite, are clearly observed. No reflections from other species indicate the obtained materials are ceria modified SBA-15. Additionally, the diffraction peaks of ceria are a little broad, and the calculated grain sizes of crystalline CeO_2 are listed in **Table 1**. In general, the mean grain sizes of ceria in CeO_2@SBA-15 samples are in the range of 6–9 nm, whereas that in CeO_2/SBA-15 only has an average size of 5 nm. The result is a little abnormal, as compare to other methods, it is generally acknowledged that the guest species prepared by impregnation technique present relatively larger particle size after been calcined (Sietsma et al., 2006; Munnik et al., 2015). One plausible explanation is that the ceria in CeO_2/SBA-15 are confined in the pore channels and as a result, their nonhomogenous aggregation is limited.

In order to get further information on the porosity of mesoporous CeO_2-silica composites and evidence of pore clogging, N_2 physisorption characterization was carried out. **Figure 4** shows the adsorption-desorption isotherms and pore size distributions (PSD) of CeO_2@SBA-15 samples as well as that of CeO_2/SBA-15. In general, all isotherms in **Figure 4A** possess a hysteresis loop at relative pressure (p/p_0) between 0.6 and 1.0, which can be filed into type IV according to IUPAC classification, indicative of the formation of mesoporous materials. This is further revealed by PSD curves (**Figure 4B**) with maximum dV/dlogw in the range between 5 and 10 nm. By comparing the patterns of CeO_2@SBA-15, it is found that the hysteresis loops are H_1 for the samples synthesized with 0.2, 0.5, and 0.8 g urea, while that of CeO_2@SBA-15(1.2) is analog to H_3 type, corresponding to less ordered mesoporous material. For CeO_2/SBA-15, the pore size is smaller than that of CeO_2@SBA-15. Moreover, it is interesting to find that there is a step-wise desorption isotherm in the desorption branch and the corresponding PSD curve presents a bimodal distribution centered at 4.0 and 5.7 nm. The phenomenon was previously reported by Van Der Voort et al. (2002), Groen et al. (2003) on the development of plugged hexagonal silicas containing both open and encapsulated mesopores. Hence, combined with wide angle XRD result, the two-step desorption can be viewed as powerful evidence of ceria nanoparticles confined in the pore channels, which in turn leads to a fake PSD at 4.0 nm. Moreover, as shown in **Table 1**, the obvious decrease in pore volume after insertion of CeO_2, together with average grain size of ceria close to pore size of CeO_2/SBA-15, are other helpful evidences for determination of CeO_2 location and its heavy clogging effect. For CeO_2@SBA-15 samples, the absence of two-step N_2 desorption demonstrates that the mesopores do not suffer from pore clogging.

Transmission electron microscopy (TEM) characterization has the advantage of providing direct observation of the ordered mesostructures as well as the distribution of guest species. **Figure 5** shows the typical TEM images of CeO_2@SBA-15 (0.8) and CeO_2/SBA-15. For both samples, the alternating clear and dark stripes are visible, indicating the formation of ordered SBA-15 framework. For CeO_2/SBA-15, small nanoparticles confined in mesopore channels are clear (**Figure 5b**). Their sizes were 5–6 nm, in good agreement with the result calculated from Sherrer equation. In contrast, no ceria particles encapsulated in the mesopore channels can be detected from **Figure 5a**, depicting the clogging-free feature of CeO_2@SBA-15.

Characterization of CuO-Loaded Catalysts

It is reported that copper-ceria catalyst is much active for catalytic removal of NO with CO (Bera et al., 1999; Hu et al., 2001; Wen and He, 2002; Pantazis and Pomonis, 2006; Liu et al., 2009). In order to investigate the catalytic performance of the synthesized materials, NO+CO was chosen as a model reaction and CeO_2@SBA-15 (0.8) was employed as a support to load CuO. For comparison, other two supports (CeO_2/SBA-15 and SBA-15) with identical CuO loading were prepared. Their physicochemical properties and catalytic performances over NO+CO reaction were characterized and results are presented and discussed in the following sections.

TABLE 1 | The physicochemical properties of the synthesized samples.

Samples	D_{CeO2} [a](nm)	S_{BET} [b](m^2/g)	a_0 [c](nm)	d_p [d](nm)	V_p [e](cm^3/g)	δ [f](nm)
SBA-15	-	800.97	10.40	5.68	1.01	4.72
CeO_2/SBA-15	5.26	588.83	10.22	5.69 [g]	0.70	4.53
CeO_2@SBA-15(0.2)	7.20	562.98	11.52	7.33	1.10	4.19
CeO_2@SBA-15(0.5)	6.44	235.12	11.66	8.90	0.70	2.76
CeO_2@SBA-15(0.8)	9.00	355.71	11.80	7.35	0.96	4.45
CeO_2@SBA-15(1.2)	7.20	383.03	11.80	7.54	1.15	4.26

[a] The average grain size of ceria. [b] BET surface area. [c] The unit-cell parameter calculated from $a_0 = d_{100} \times 2/3^{1/2}$. [d] BJH mesopore diameter. [e] Total pore volume. [f] Pore wall thickness calculated from $\delta = a_0 - d_p$. [g] The fake d_p centered at 4.0 nm was not filed.

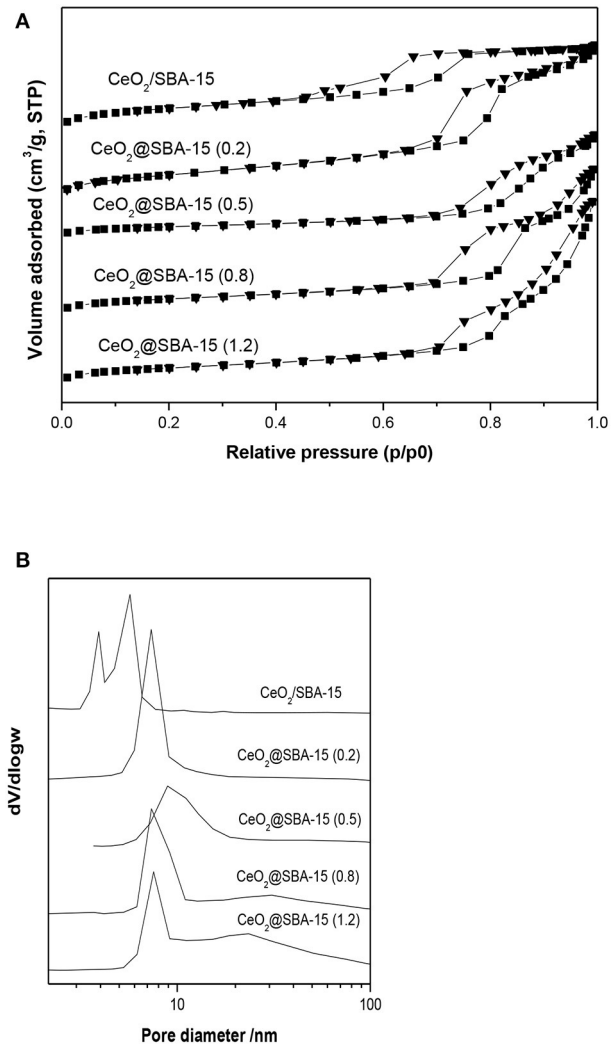

FIGURE 4 | The N_2 sorption isotherms **(A)** and pore size distributions **(B)** of various ceria loaded samples.

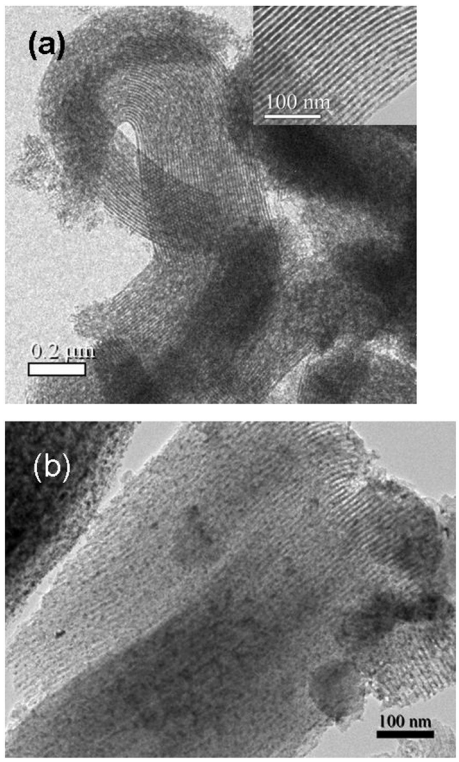

FIGURE 5 | Typical TEM images of **(a)** CeO_2@SBA-15 (0.8) (inset: the high magnification image) and **(b)** CeO_2/SBA-15.

XRD Results

The small angle XRD patterns of CuO-loaded samples are displayed in **Figure 6**. In general, both CuO/SBA-15 and CuO/CeO_2@SBA-15 exhibit three reflections, indicating the well-ordered mesoporous structures are preserved after loaded with CuO. Comparing to that of CuO/SBA-15, the intensities of (100) diffraction peak is severely weakened and those of (110) and (200) become faint for CuO/CeO_2/SBA-15, implying that multiple impregnations could induce a deterioration effect on the ordering of mesoporous structures.

The wide angle XRD patterns of CuO-loaded samples are shown in **Figure 7**. Similar to the results of CuO free samples, all the patterns present a broad peak at $2\theta = 20–26^\circ$ which is assigned to amorphous silica. Besides the broad peak, the rest of diffraction peaks in CuO/SBA-15 are characteristic of crystalline CuO. For the patterns of samples with ceria modification, the characteristic peaks belong to crystalline CeO_2 are present besides those of crystalline CuO and their

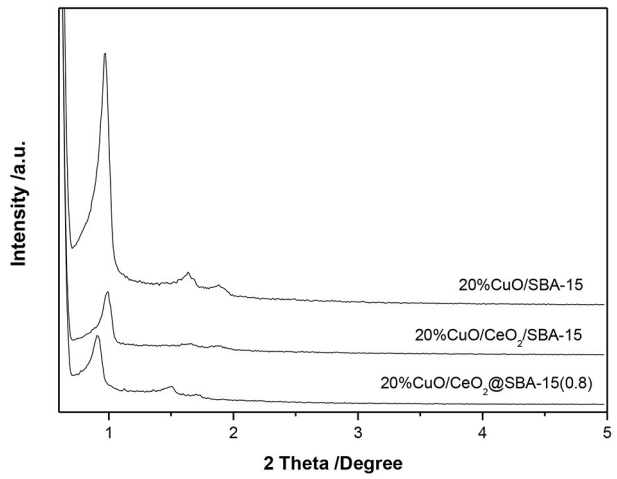

FIGURE 6 | The small angle XRD patterns of three CuO-loaded catalysts.

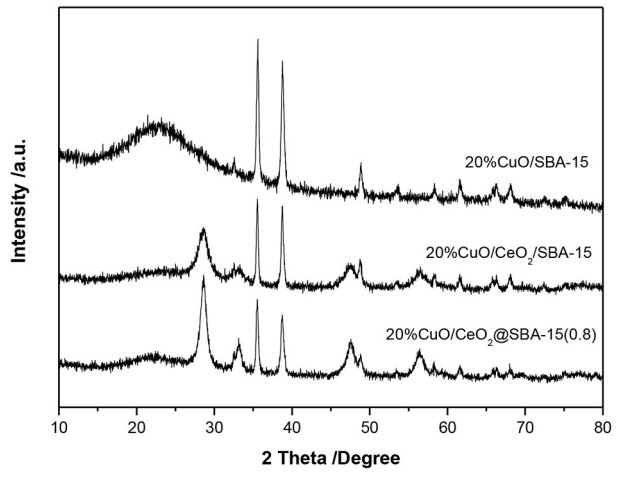

FIGURE 7 | The wide angle XRD patterns of three CuO-loaded catalysts.

intensities are comparable to those of CuO free samples. To further investigate the most intense diffraction peaks (2θ = 35.6°, 38.8°), it is observed that their intensities decreased in the following order: CuO/SBA-15, CuO/CeO_2/SBA-15, and CuO/CeO_2@SBA-15. Generally, X-ray diffraction intensity is an effective indicator of guest species dispersion. The weaker the reflection is, the higher the dispersion is achieved. In the present case, with the introduction of ceria onto silica matrix, the dispersion of CuO is improved. This can be well accounted by the fact that ceria is more capable of dispersing CuO (Dong et al., 1997). Furthermore, to explore the different dispersion behaviors between the two ceria modified samples, we should bear in mind that the location of ceria particles is not the same. Based on the results of N_2 sorption and TEM, it is known that certain amounts of ceria are in the pore channels for CeO_2/SBA-15, whereas most of the ceria are dispersed on the surface of the silica matrix in CeO_2@SBA-15. By calculating with Scherrer equation for the samples, the average particle sizes of CuO are all larger than 20 nm. It is a useful indication that crystalline CuO are dispersed on the external surface. Despite the same loading of ceria for the two samples, a significant part of ceria are encapsulated in the pore channels. As a result, only a small part of ceria on the external surface is in contact with CuO and takes the role of dispersing CuO. Based on this discussion, it is reasonable to suppose that the difference in ceria location contributes to the different dispersion behavior of CuO in the two ceria-contained catalysts.

H_2-TPR Results

H_2-TPR profiles for various CuO-loaded catalysts are shown in **Figure 8**. These profiles show several features: (i) all of the three profiles present two reduction peaks, which can be classified into the reduction of highly dispersed and crystalline CuO (Luo et al., 1997; Zheng et al., 2005; Parida and Rath, 2007). By comparing the H_2 consumptions, it is known that crystalline CuO are dominant. This is consistent with the wide angle XRD result. (ii) The peak value corresponding to maximum H_2 consumption varies for different samples. The two peaks at 226 and 305°C in CuO/SBA-15 shift to lower values with modification of ceria. This is probably due to the outstanding oxygen storage capacity (OSC) and ease of the Ce(III)-Ce(IV) redox cycle of ceria (Fan et al., 2013). Possessing these unique properties, ceria can greatly improve the redox properties of CuO (Luo et al., 1997; Colliard and Nyman, 2021). Hence, the reducibility of CuO is improved and the corresponding peaks shift to lower values. Base on this analysis, it is reasonable to understand that the peak values of CuO/CeO_2/SBA-15 are a little higher than those of CuO/CeO_2@SBA-15. For CuO/CeO_2@SBA-15, more ceria are available to interact with CuO and as a result, their promoting effect is more notable. Hence, the results of H_2-TPR are closely related to the presence and location of ceria, which in turn confirms the different locations of ceria by the two different methods.

Catalytic Activity Results

The NO conversion and N_2 selectivity as a function of reaction temperature were studied and results are shown in **Figure 9**. These results show several features: (i) generally, the activity (NO conversion and N_2 selectivity) increases with temperature rising. The catalysts display low NO conversions and N_2 selectivity at relatively low temperature (200°C). When the reaction temperature reaches 350°C, all of the catalysts exhibit excellent activity, with the NO conversions exceeding 90% and N_2 selectivity exceeding 85%. (ii) The activities of the ceria modified catalysts are better than that of CuO/SBA-15. (iii) At every point, the catalytic activity of CuO/CeO_2@SBA-15 is the best among the three catalysts. It displays a NO conversion of 83.9% with N_2 selectivity of 84.6% at moderate temperature (250°C), whereas the other two catalysts only achieve the NO conversions less than 20% and N_2 selectivity less than 30%.

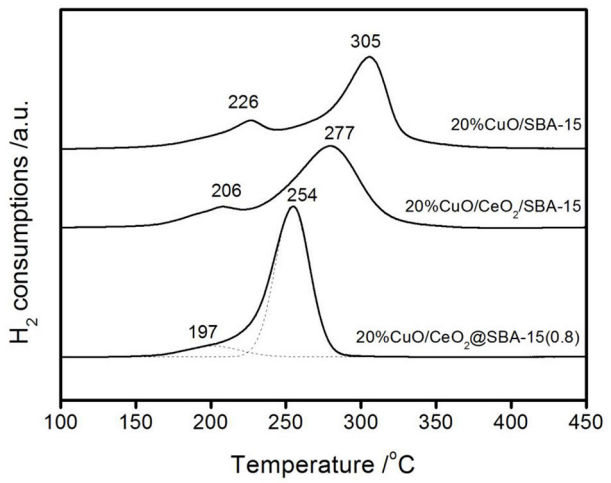

FIGURE 8 | The H_2-TPR profile of three CuO-loaded catalysts.

By correlating H_2-TPR results with catalytic performances, some useful information can be distilled regarding the activity variations in the catalysts. As reported in literature (Hu et al., 2001), the NO+CO reaction over copper-based catalysts was proposed to proceed in the following cycling:

$$CO + CuO - - - - - - Cu^{+}/Cu^{0} + CO_2 \quad (1)$$

$$Cu^{+}/Cu^{0} + NO(\text{adsorbednitrite, nitrate}) - - - - - - Cu^{2+} + N_2O + N_2 \quad (2)$$

The cycling process is intimately related to redox properties of the catalysts. From H_2-TPR patterns, it is known that two different copper species are present in the three catalysts: highly dispersed and the dominant crystalline CuO. At the operation temperature of 250°C, both highly dispersed and crystalline CuO take part in the catalytic cycling, and resultantly, the catalytic performance was excellent. On the other hand, the catalytic performances of the other two catalysts show relatively low NO conversions and N_2 selectivity. The reason may be that only highly dispersed CuO is participated in the catalytic cycling, while that of crystalline CuO is partial or totally not involved. This inference is further supported by the performances of the other two catalysts at the neighboring higher temperature (275°C). At that temperature, the less reducible crystalline CuO can be reduced by CO. Accordingly, the critical cycling process is turned on and their catalytic activities are greatly enhanced.

CONCLUSIONS

In the paper, a facile one-pot method was reported for the preparation of CeO_2 modified SBA-15 without pore clogging. The presence of cerium could induce assembly of ordered mesoporous silica and ceria were *in situ* grafted onto mesoporous silica matrix with the aid of urea decomposition. The contents of ceria in the samples, together with ordering of the mesostructures, were much affected by the amount of urea added. By comparing the one-pot synthesis with that of the conventional impregnation method, besides facile and green operation, it was found that the textural property and ceria location of the final product were not the same. The silica matrix with larger pore size is presented by the one-pot synthetic method, whereas the impregnation method is characterized by confined ceria in mesopore channels. After loaded with CuO, the ordered mesoporous structure was still preserved. The dispersion and redox properties of CuO were correlated with the presence and location of ceria, which in turn determined their catalytic performances in NO+CO reaction. Since no pore clogging is observed for CeO_2@SBA-15, more chance is present for ceria to interact with CuO. As such, the ceria promotion effect was more prominent and much better catalytic performance is obtained.

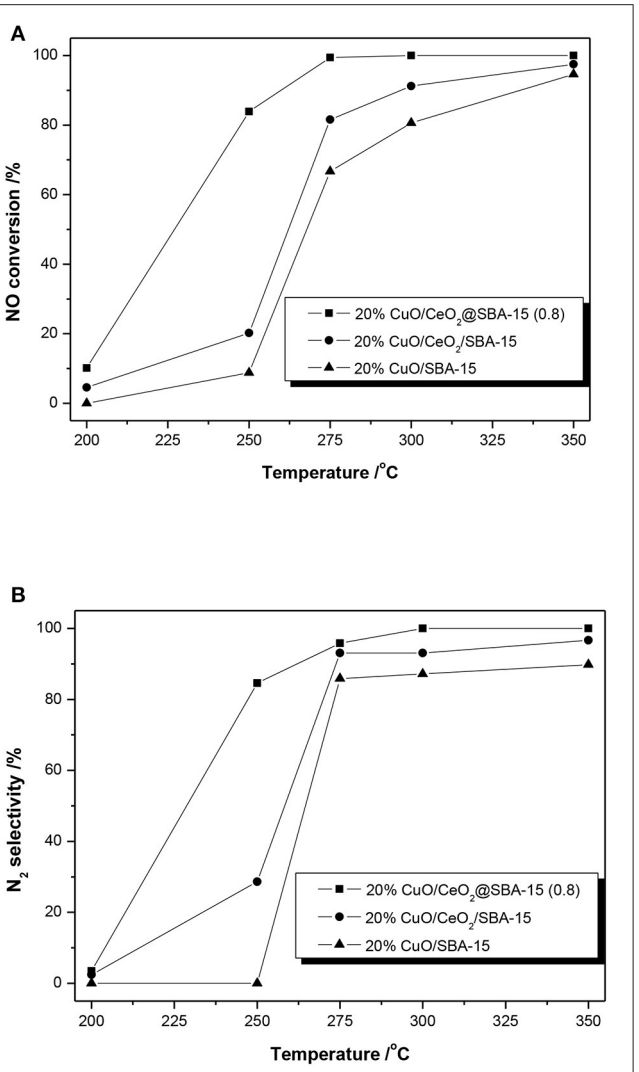

FIGURE 9 | Results of **(A)** NO conversion and **(B)** N_2 selection over CuO-loaded catalysts as a function of reaction temperatures.

DATA AVAILABILITY STATEMENT

The original contributions presented in the study are included in the article/**Supplementary Material**, further inquiries can be directed to the corresponding author/s.

AUTHOR CONTRIBUTIONS

KM: methodology, validation, investigation, writing—original draft. LD: project administration. CT: conceptualization, writing—review and editing, funding acquisition. HZ: conceptualization, writing—review, editing. All authors contributed to the article and approved the submitted version.

ACKNOWLEDGMENTS

The authors gratefully acknowledge the financial support from the Major Scientific and Technological Project of Bingtuan (2018AA002) and National Natural Science Foundation of China (21773106, 21976081).

SUPPLEMENTARY MATERIAL

The Supplementary Material for this article can be found online at: https://www.frontiersin.org/articles/10.3389/fenvc.2021.670431/full#supplementary-material

REFERENCES

Akondi, A. M., Trivedi, R., Sreedhar, B., Kantama, M. L., and Bhargav, S. (2012). Cerium-containing MCM-41 catalyst for selective oxidative arene cross-dehydrogenative coupling reactions. *Catal. Today* 198, 35–44. doi: 10.1016/j.cattod.2012.05.029

Bera, P., Aruna, S. T., Patil, K. C., and Hegde, M. S. (1999). Studies on Cu/CeO_2: a new NO reduction catalyst. *J. Catal.* 186, 36–44. doi: 10.1006/jcat.1999.2532

Bi, F., Zhang, X., Xiang, S., and Wang,Y. (2020). Effect of Pd loading on ZrO2 support resulting from pyrolysis of UiO-66: application to CO oxidation. *J. Colloid Interf. Sci.* 573, 11–20. doi: 10.1016/j.jcis.2020.03.120

Bi, Y. D., Zhang, W., Xu, H. Y., and Li, W. Z. (2007). Nanocrystalline CeO_2 in SBA-15: performance of Pt/CeO_2/SBA-15 catalyst for water-gas-shift reaction. *Catal. Lett.* 119, 126–133. doi: 10.1007/s10562-007-9209-3

Colliard, I., and Nyman, M. (2021). Ce^{IV}_{70} oxosulfate rings, frameworks, supramolecular assembly, and redox activity. *Angew. Chem. Int. Ed.*, 60, 7308–7315. doi: 10.1002/anie.202016522

Corma, A., Chane-Ching, J. Y., Airiau, M., and Martinez, C. (2004). Synthesis and catalytic properties of thermally and hydrothermally stable, high-surface-area SiO_2-CeO_2 mesostructured composite materials and their application for the removal of sulfur compounds from gasoline. *J. Catal.* 224, 441–448. doi: 10.1016/j.jcat.2004.03.004

Dong, L., Jin, Y. S., and Chen, Y. (1997). Dispersion state of CuO on CeO_2–an incorporation model for the interaction between metal oxide and oxide support. *Sci. China Ser. B Chem.* 40, 24–30. doi: 10.1007/BF02882184

Escas, V., Delahaye, E., Imperor-Clerc, M., Beaunier, P., Appay, M. D., and Davidson, A. (2007). Modifying the porosity of SBA-15 silicas by post-synthesis basic treatments. *Micropor. Mesopor. Mater.* 102, 234–241. doi: 10.1016/j.micromeso.2006.12.049

Fan, L. D., Wang, C. Y., Chen, M. M., and Zhu, B. (2013). Recent development of ceria-based (nano) composite materials for low temperature ceramic fuel cells and electrolyte-free fuel cells. *J. Power Sour.* 234, 154–174. doi: 10.1016/j.jpowsour.2013.01.138

Groen, J. C., Peffer, L. A. A., and Perez-Ramirez, J. (2003). Pore size determination in modified micro- and mesoporous materials. Pitfalls and limitations in gas adsorption data analysis. *Micropor. Mesopor. Mater.* 60, 1–17. doi: 10.1016/S1387-1811(03)00339-1

Hu, Y. H., Dong, L., Shen, M. M., Liu, D., Wang, J., Ding, W. P., et al. (2001). Influence of supports on the activities of copper oxide species in the low-temperature NO+CO reaction, *Appl. Catal. B Environ.* 31, 61–69. doi: 10.1016/S0926-3373(00)00269-1

Khalil, K. M. S. (2007). Cerium modified MCM-41 nanocomposite materials via a nonhydrothermal direct method at room temperature. *J. Colloid Interface Sci.* 315, 562–568. doi: 10.1016/j.jcis.2007.07.030

Krishnan, C. K., Hayashi, T., and Ogura, M. (2008). A new method for post-synthesis coating of zirconia on the mesopore walls of SBA-15 without pore blocking. *Adv. Mater.* 20, 2131–2136. doi: 10.1002/adma.200702822

Li, J. S., Hao, Y. X., Li, H. J., Xia, M. Y., Sun, X. Y., and Wang, L. J. (2009). Direct synthesis of CeO_2/SiO_2 mesostructured composite materials via sol-gel process, *Micropor. Mesopor. Mater.* 120, 421–425. doi: 10.1016/j.micromeso.2008.12.014

Li, Y., and Shen, W. J. (2014). Morphology-dependent nanocatalysts: rod-shaped oxides. *Chem. Soc. Rev.* 43, 1543–1574. doi: 10.1039/C3CS60296F

Liang, X., Wang, X., Zhuang, Y., Xu, B., Kuang, S. M., and Li, Y. D. (2008). Formation of CeO_2-ZrO_2 solid solution nanocages with controllable structures via Kirkendall effect. *J. Am. Chem. Soc.* 130, 2736–2737. doi: 10.1021/ja7109629

Liu, L. J., Liu, B., Dong, L. H., Zhu, J., Wan, H. Q., Sun, K. Q., et al. (2009). *In situ* FT-infrared investigation of CO or/and NO interaction with $CuO/Ce_{0.67}Zr_{0.33}O_2$ catalysts. *Appl. Catal. B Environ.* 90, 578–586. doi: 10.1016/j.apcatb.2009.04.019

Luo, M. F., Ma, J. M., Lu, J. Q., Song, Y. P., and Wang, Y. J. (2007). High-surface area CuO-CeO_2 catalysts prepared by a surfactant-templated method for low-temperature CO oxidation. *J. Catal.* 246, 52–59. doi: 10.1016/j.jcat.2006.11.021

Luo, M. F., Zhong, Y. J., Yuan, X. X., Zheng, X. M. (1997). TPR and TPD studies of CuO/CeO_2 catalysts for low temperature CO oxidation. *Appl. Catal. A Gen.* 162, 121–131. doi: 10.1016/S0926-860X(97)00089-6

Ma, K. L., Zou, W. X., Zhang, L., Li, L. L., Yu, S. H., Tang, C. J., et al. (2017). Construction of hybrid multi-shell hollow structured CeO_2-MnO*x* materials for selective catalytic reduction of NO with NH_3. *RSC Adv.* 7, 5989–5999. doi: 10.1039/C6RA25863H

Mikheeva, N. N., Zaikovskii, V. I., and Mamontov, G. V. (2019). Synthesis of ceria nanoparticles in pores of SBA-15: pore size effect and influence of citric acid addition, *Micropor. Mesopor. Mater.* 277, 10–16. doi: 10.1016/j.micromeso.2018.10.013

Munnik, P. E., de Jongh, K. P., de Jong (2015). Recent developments in the synthesis of supported catalysts. *Chem. Rev.* 115, 6687–6718. doi: 10.1021/cr500486u

Pantazis, C. C., and Pomonis, P. J. (2006). Synthesis of highly loaded Cu/Ce mesoporous silica. active catalyst for the simultaneous reduction of SO_2 and NO with CO. *Chem. Commun.* 12, 1268–1270. doi: 10.1039/b516450h

Parida, K. M., and Rath, D. (2007). Structural properties and catalytic oxidation of benzene to phenol over CuO-impregnated mesoporous silica. *Appl. Catal. A Gen.* 321, 101–108. doi: 10.1016/j.apcata.2007.01.054

Qi, L., Yu, Q., Dai, Y., Tang, C. J., Liu, L. J., Zhang, H. L., et al. (2012). Influence of cerium precursors on the structure and reducibility of mesoporous CuO-CeO_2 catalysts for CO oxidation. *Appl. Catal. B Environ.* 119, 308–320. doi: 10.1016/j.apcatb.2012.02.029

Ri, S. H., Bi, F., Guan, A., and Zhang, X. D. (2021). Manganese-cerium composite oxide pyrolyzed from metal organic framework supporting palladium nanoparticles for efficient toluene oxidation. *J. Colloid Interf. Sci.* 586, 836–846. doi: 10.1016/j.jcis.2020.11.008

Shen, W. H., Dong, X. P., Zhu, Y. F., Chen, H. R., and Shi, J. L. (2005). Mesoporous CeO_2 and CuO-loaded mesoporous CeO_2: synthesis, characterization, and CO catalytic oxidation property. *Micropor. Mesopor. Mater.* 85, 157–162. doi: 10.1016/j.micromeso.2005.06.006

Shi, Y. J., Wang, J. L., and Zhou, R. X. (2021). Pt-support interaction and nanoparticle size effect in Pt/CeO_2-TiO_2 catalysts for low temperature VOCs removal. *Chemosphere* 265:129127. doi: 10.1016/j.chemosphere.2020.129127

Sietsma, J. R. A., van Dillen, A. J., de Jongh, P. E., and de Jong, K. P. (2006). Application of ordered mesoporous materials as model supports to study catalyst preparation by impregnation and drying, *Stud. Surf. Sci. Catal.*, 162, 95–102. doi: 10.1016/S0167-2991(06)80895-5

Slavinskaya, E. M., Zadesenets, A. V., Stonkus, O. A., Stadnichenko, A. I., Shchukarev, A. V., Yu,.V., and Shubin, S. V. (2020). Thermal activation of Pd/CeO_2-SnO_2 catalysts for low-temperature CO oxidation. *Appl. Catal. B Environ.* 277:119275. doi: 10.1016/j.apcatb.2020.119275

Ta, N., Liu, J. Y., Chenna, S., Crozier, P. A., Li, Y., Chen, A. L., et al. (2012). Stabilized gold nanoparticles on ceria nanorods by strong interfacial anchoring. *J. Am. Chem. Soc.* 134, 20585–20588. doi: 10.1021/ja310341j

Tang, C. J., Li, J. C., Yao, X. J., Sun, J. F., Cao, Y., Zhang, L., et al. (2015). Mesoporous NiO-CeO_2 catalysts for CO oxidation: nickel content effect and mechanism aspect. *Appl. Catal. A Gen.* 494, 77–86. doi: 10.1016/j.apcata.2015.01.037

Tang, C. J., Zhang, H. L., and Dong, L. (2016). Ceria-based catalysts for low-temperature selective catalytic reduction of NO with NH_3. *Catal. Sci. Technol.*, 6, 1248–1264. doi: 10.1039/C5CY01487E

Trovarelli, A., and Llorca, J. (2017). Ceria catalysts at nanoscale: how do crystal shapes shape catalysis. *ACS Catal.* 7, 4716–4735. doi: 10.1021/acscatal.7b01246

Van Der Voort, P., Ravikovitch, P. I., De Jong, K. P., Neimark, A. V., Janssen, A. H., Benjelloun, M., et al. (2002). Vansant, Plugged hexagonal templated silica: a unique micro- and mesoporous composite material with internal silica nanocapsules. *Chem. Commun.* 1010–1011. doi: 10.1016/S0167-2991(02)80523-7

Wang, Y. H., Xie, Y. Y., Zhang, C. S., Chen, W. J., Wang, J., Zhang, R. Q., et al. (2021). Tuning the oxygen mobility of CeO_2 via Bi-doping for diesel soot oxidation: experimental and DFT studies. *J. Environ. Chem. Eng.* 9:105049. doi: 10.1016/j.jece.2021.105049

Wei, Y. C., Liu, J., Zhao, Z., Duan, A. J., Jiang, G. Y., Xu, C. M., et al. (2011). Three-dimensionally ordered macroporous $Ce_{0.8}Zr_{0.2}O_2$-supported gold nanoparticles: synthesis with controllable size and super-catalytic performance for soot oxidation, *Energy Environ. Sci.* 4, 2959–2970. doi: 10.1039/c0ee00813c

Wen, B., and He, M. Y. (2002). Study of the Cu-Ce synergism for NO reduction with CO in the presence of O_2, H_2O and SO_2 in FCC operation. *Appl. Catal. B Environ.* 37, 75–82. doi: 10.1016/S0926-3373(01)00316-2

Wu, C. Z., Dang, Z. Y., Prato, M., Marras, S., Cerea, A., Angelis, F. D., et al. (2018). Nanosized, hollow, and Mn-doped CeO_2/SiO_2 catalysts via galvanic replacement: preparation, characterization, and application as highly active catalysts. *ACS Appl. Nano. Mater.* 1, 1438–1443. doi: 10.1021/acsanm.7b00380

Zhan, S. H., Zhang, H., Zhang, Y., Shi, Q., Li, Y., and Li, X. J. (2017). Efficient NH_3-SCR removal of NO*x* with highly ordered mesoporous $WO_3(\chi)$-CeO_2 a t low temperatures. *Appl. Catal. B Environ.* 203, 199–209. doi: 10.1016/j.apcatb.2016.10.010

Zhang, H. L., Tang, C. J., Sun, C. Z., Qi, L., Gao, F., Dong, L., et al. (2012). Direct synthesis, characterization and catalytic performance of bimetallic Fe-Mo-SBA-15 materials in selective catalytic reduction of NO with NH_3. *Micropor. Mesopor. Mater.* 151, 44–55. doi: 10.1016/j.micromeso.2011.11.018

Zheng, X. C., Wang, S. P., Wang, S. R., Zhang, S. M., Huang, W. P., and Wu, S. H. (2005). Preparation, characterization and catalytic properties of CuO/CeO_2 system. *Mater. Sci. Eng.* 25, 516–520. doi: 10.1016/j.msec.2005.03.005

Conflict of Interest: The authors declare that the research was conducted in the absence of any commercial or financial relationships that could be construed as a potential conflict of interest.

Copyright © 2021 Ma, Zhang, Tang and Dong. This is an open-access article distributed under the terms of the Creative Commons Attribution License (CC BY). The use, distribution or reproduction in other forums is permitted, provided the original author(s) and the copyright owner(s) are credited and that the original publication in this journal is cited, in accordance with accepted academic practice. No use, distribution or reproduction is permitted which does not comply with these terms.